Noise-Domain Reflectometry for Locating Wiring Faults

Chet Lo, *Member, IEEE,* and Cynthia Furse, *Senior Member, IEEE*

***Abstract*—Reflectometry is commonly used to determine the integrity of cables and wiring. This paper describes a new family of reflectometers, the noise-domain reflectometers (NDR), that uses existing data signals on wiring and does not need to generate any signals of their own. There are two types of NDR, type I (where incident and reflected signals are separated) and type II (where they are superimposed). NDR is totally "quiet" and passive to other signals on the media. Especially for NDR II, detection can be done totally nonintrusively. In this paper, the working principles of NDR are described. Simulation results and examples for location of faults to within 3 inches on wiring up to 180 feet are provided.**

***Index Terms*—Aging wire fault location, correlation, reflectometry, wire fault detection.**

I. Introduction

REFLECTOMETRY is commonly used to test the integrity of wires and cables [1]. Time-domain reflectometry (TDR) [2]–[5] sends a step or pulse of voltage down the wire, which reflects at any impedance discontinuity such as a break or short circuit in the wire. The reflected signal is detected at the source end. The delay between the incident and reflected signals tells how long the wire is, and the magnitude and polarity of the reflected signal tells the magnitude and type of fault. Frequency-domain reflectometry (FDR) [6] sends a set of stepped frequency sine waves down the wire and measures the phase difference between incident and reflected sine waves. These methods are accurate, however they cannot easily be used on live wires. More recently, spread-spectrum TDR (STDR or SSTDR) [7]–[9] has been developed. This method sends a digital pseudonoise (PN) code or sine wave modulated PN code down the wire and utilizes correlation to detect the time delay between the incident and reflected signals and thus the length of the wire. The spread-spectrum technique is excellent for testing live wires, because the magnitude of the PN code can be small enough to not interfere with the signal already on the wire. It is very immune to noise both from the existing signal and other noise sources. It has been shown [7] that by testing the wire when it is live, small arcs (intermittent shorts) can be located during the few milliseconds they are active rather than waiting until after the aircraft is on the ground when the arc fault is typically a much smaller impedance discontinuity and is therefore extremely difficult or impossible to detect. Testing live also allows a dynamic baseline to be collected. Smaller impedance discontinuities can be detected by examining the difference between the baseline and a later (but not much later) signal.

This paper introduces another method for testing live wires, which functions very similar to spread-spectrum methods by utilizing correlation to determine the length of the wire. However, unlike spread-spectrum methods that require a PN code as the test signal, any significant noise or high-speed signal already on the line can be used to passively test the wire and locate the distance to a fault. The family of noise-domain reflectometers (NDR) utilizes the properties of time domain autocorrelation functions and can be used to determine individual time delays or multiple reflections such as from branched networks. The advantage of using NDR over other forms of reflectometry is that there is no need to transmit a specific test signal. Instead, the existing signal or noise on the wire is used as the test signal. In other words, NDR can be totally "quiet" to other users of the media being tested. Thus, NDR may be ideal for applications where data integrity is critical such as in flight "live" wire fault location for aging aircraft wiring or applications where stealth is desired.

II. Background

NDR is developed based on the properties of the autocorrelation functions of test signals used in reflectometry. A brief review of autocorrelation functions is given here, and a more complete discussion can be found in [10]. The autocorrelation function effectively measures how similar or different two functions are. For our application, it will have a peak when the incident and reflected signals are synchronized, and low values when they are not. The time delay required to produce this synchronization will be the time delay for the signal propagating to and returning from a fault. Knowing the velocity of propagation (VOP) on the cable, the distance to the fault can then be found. The VOP on most aircraft wiring is 0.55– 0.7 times the speed of light, depending on the type and gauge of wiring. Variation is highest among unshielded, bundled wires. Our testing has shown variation up to 3% within a bundle of 128 wires, for instance. Any errors in VOP directly effect the length measurements [11].

Manuscript received August 1, 2003; revised June 22, 2004. This work was supported in part by the National Science Foundation under Grant ECS-0115157, and in part by the Utah State Center of Excellence Program.

The authors are with the Department of Electrical and Computer Engineering, University of Utah, Salt Lake City, UT 84112 USA (e-mail: clo@ece.utah.edu; cfurse@ece.utah.edu).

Digital Object Identifier 10.1109/TEMC.2004.842109

Let random signal $f(t)$ have unit power, that is $\lim_{T\to\infty}(1/2T)\int_{-T}^{T} f^2(t)dt = 1$. Then the autocorrelation function of $f(t)$ can be defined as

$$\begin{aligned}\phi_f(\tau) = &\lim_{T\to\infty}\frac{1}{2T-|\tau|}\\ &\times\int_{-T+\frac{|\tau|}{2}}^{T-\frac{|\tau|}{2}}\int_{-\infty}^{\infty}\int_{-\infty}^{\infty} f\left(t+\frac{\tau}{2}\right)f\left(t-\frac{\tau}{2}\right)\\ &\times p\left(f\left(t+\frac{\tau}{2}\right),f\left(t\frac{\tau}{2}\right)\right)\\ &\times df\left(t+\frac{\tau}{2}\right)df\left(t-\frac{\tau}{2}\right)dt \end{aligned} \tag{1}$$

where $f(t+(\tau/2))$ and $f(t-(\tau/2))$ are treated as random variables for given t and τ, and $p(f(t+(\tau/2)), f(t-(\tau/2)))$ is their joint probability density function. If $f(t)$ is a deterministic signal, $p(f(t+(\tau/2)), f(t-(\tau/2)))$ becomes a delta function. Then (1) becomes

$$\phi_f(\tau) = \lim_{T\to\infty}\frac{1}{2T-|\tau|}\int_{-T+\frac{|\tau|}{2}}^{T-\frac{|\tau|}{2}} f\left(t+\frac{\tau}{2}\right)f\left(t-\frac{\tau}{2}\right)dt. \tag{2}$$

For this application, it is safe to assume that the signal, $f(t)$, is deterministic. At the same time, to simplify the discussion, $f(t)$ will also be assumed to have zero mean, which is typical of most but not all aircraft signals and their noise.

An important idea required in the development of NDR is shift uncorrelation of a function. By definition, if $f(t)$ is shift uncorrelated then $\phi_f(\tau) = \delta(\tau)$. In other words, $\phi(\tau)$ will be large when $\tau = 0$ and zero when $\tau \neq 0$ (the function is uncorrelated with its time shifted echo). From (1) and (2), $\phi_f(\tau)$ is only determined after integration over all time from negative infinity to positive infinity. However, in practice, $f(t)$ is only available for a finite length of time, T. T needs to be large enough to provide a good autocorrelation function and small enough to capture an intermittent fault on the wire. If T is large compared to the time variation in $f(t)$, then the autocorrelation can be estimated as

$$\phi_{f_T}(\tau) = \frac{1}{2T-|\tau|}\int_{-T+\frac{|\tau|}{2}}^{T-\frac{|\tau|}{2}} f\left(t+\frac{\tau}{2}\right)f\left(t-\frac{\tau}{2}\right)dt \approx \phi_f(\tau). \tag{3}$$

If $f(t)$ is shift uncorrelated, $\phi_{f_T}(\tau)$ will be "small" when $\tau \neq 0$ and "large" when $\tau = 0$, even when T is relatively small. Thus, the more random or noisy, and the higher the bandwidth of the signal on the wire, $f(t)$, the better NDR can detect faults in the shortest amount of time. If the integration time T is significantly longer than the time delay τ, the autocorrelation function can be further simplified as

$$\begin{aligned}\phi_{f_T} &= \frac{1}{2T-|\tau|}\int_{-T+\frac{|\tau|}{2}}^{T-\frac{|\tau|}{2}} f\left(t+\frac{\tau}{2}\right)f\left(t-\frac{\tau}{2}\right)dt\\ &= \frac{1}{2T-|\tau|}\int_{-T+\frac{|\tau|}{2}-\frac{\tau}{2}}^{T-\frac{|\tau|}{2}-\frac{\tau}{2}} f(t)f(t-\tau)dt\\ &\approx \frac{1}{2T}\int_{-T}^{T} f(t)f(t-\tau)dt \end{aligned} \tag{4}$$

which simplifies the following presentation.

Another important idea required in the development of NDR is the time invariance of a shift uncorrelated function. Defining $g(t) = f(t-\lambda)$ (a time delayed copy of $f(t)$), then $g(t-\tau) = f(t-(\lambda+\tau))$, and

$$\begin{aligned}\phi_{g_T}(\tau) &= \frac{1}{2T}\int_{-T}^{T} g(t)g(t-\tau)dt\\ &= \frac{1}{2T}\int_{-T}^{T} f(t-\lambda)f\left(t-(\lambda+\tau)\right)dt\\ &= \frac{1}{2T}\int_{-T-\lambda}^{T-\lambda} f(t)f(t-\tau)dt. \end{aligned} \tag{5}$$

Assuming that $f(t)$ is time invariant ("behaves" the same as time advances), the autocorrelation can be approximated as

$$\begin{aligned}\phi_{g_T}(\tau) &= \frac{1}{2T}\int_{-T-\lambda}^{T-\lambda} f(t)f(t-\tau)dt\\ &\approx \frac{1}{2T}\int_{-T}^{T} f(t)f(t-\tau)dt\\ &= \phi_{f_T}(\tau). \end{aligned} \tag{6}$$

So, if $f(t)$ is shift uncorrelated, so is $g(t)$, and both of them have similar autocorrelation functions.

The importance of this conclusion to our application is this: There is a signal $X(t)$ on the media (wire) being tested. There is no control over the generation of $X(t)$; however, it may be used as the reflectometry test signal, since $X(t)$ will travel down the wire and reflect off impedance discontinuities. In practice, $X(t)$ will be running for a long time relative to the testing process. For different t, $X(t)$ appears random. It is reasonable to assume $X(t)$ is shift uncorrelated. (From an Information Theory point of view, this means $X(t)$ is carrying meaningful information.)

Since $X(t)$ can only be observed (integrated) for a finite length of time, T, NDR is effectively working with sections of $X(t)$. These sections are $X(t)$ in sliding windows of time, each with lengths equal to or less than $2T$. These sections of $X(t)$ are $f(t)$, $g(t)$, etc. as in (5), and can be called $\{f_i(t)\}$ in

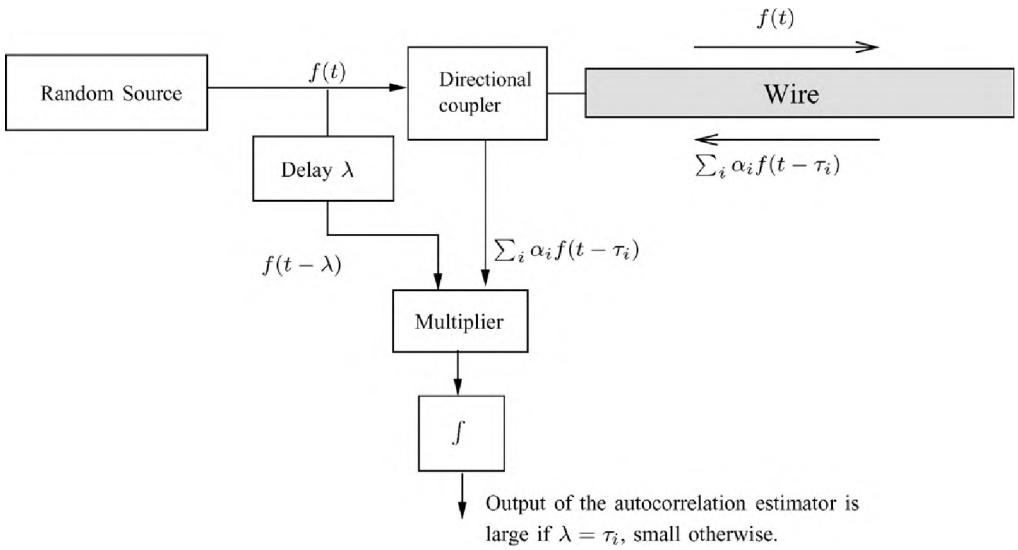

Fig. 1. NDR I block diagram.

a more systematic notation. Since they have finite lengths, they are deterministic.

$X(t)$ being shift uncorrelated implies that $\{f_i(t)\}$ is statistically shift uncorrelated. This means individual $f_i(t)$ are not necessary shift uncorrelated, but as a group, most of the $\{f_i(t)\}$ signals are "shift uncorrelated" in the sense that $\phi_{f_{i_T}}(\tau) \approx \delta(\tau)$.

Furthermore, from (6) there is some function $\phi_{f_T}(\tau)$ such that $\phi_{f_{i_T}}(\tau)$ are equivalent for all i. i.e., $\phi_{f_{i_T}}(\tau) \approx \phi_{f_T}(\tau)$. However, this approximation just means that $\phi_{f_T}(\tau)$ and $\phi_{f_{i_T}}(\tau)$ have similar behavior. In other words

$$\lim_{\Gamma\to\infty} \frac{1}{2\Gamma} \int_{-\Gamma}^{\Gamma} \left[\phi_{f_T}(\tau) - \phi_{f_{i_T}}(\tau)\right] d\tau = 0 \tag{7}$$

for all i. Thus, for any signal with significant noise or noise type behavior during the testing period (a few ms), the correlation of this signal and the reflections that occur naturally on the line gives a correlation pattern with a spike or peak indicating the location of each reflection. Multiple reflections occur on networks of cables, and each reflection can be seen independently.

III. Basic Assumption and Working Principle of NDR

There are two basic types of NDR, type I and type II. For both types, the test signal is assumed to be shift uncorrelated. At a particular position of the wire being tested, a copy of the testing signal, $f(t)$, and its reflections are available. There may be multiple paths for these reflections such as on branched networks and hence multiple time delays τ. The reflections may be represented as $\sum_i \alpha_i f_i(t-\tau_i)$, where α_i and τ_i are the attenuation (a combined effect from the magnitude of the reflection coefficient and actual loss on the wire) and the time delay respectively for the ith path of reflection.

A. Type I

For NDR I, shown in Fig. 1, separate copies of the testing signal and its reflections are needed. This can be obtained using a directional coupler (although in practice this would place a limit on the bandwidth and hence the accuracy of the tests). A delay λ is introduced during the testing. Then, a manually delayed signal is multiplied with the reflections, and integrated for a length of time T. As the value of λ is increased gradually, peaks are observed at the output of the integrator when λ matches the path delays, τ_i, of the reflections. The integrator and the multiplier form an autocorrelation estimator, and the output of the integrator is equivalent to the output of the autocorrelation estimator.

Mathematically, this is presented as

$$\begin{aligned} I &= \int_{-T+\lambda}^{T+\lambda} f(t-\lambda)\left[\sum_i \alpha_i f_i(t-\tau_i)\right] dt \\ &= \sum_i \alpha_i \int_{-T+\lambda}^{T+\lambda} f(t-\lambda) f_i(t-\tau_i) dt \\ &= 2T \sum_i \alpha_i \phi_{f_T}(\tau_i - \lambda) \end{aligned} \tag{8}$$

where I is the autocorrelation estimator output. For a shift uncorrelated testing signal, $\phi_f(\tau) = \delta(\tau)$, and $I = 2T\sum_i \alpha_i \delta(\tau_i - \lambda)$. That is, when λ is not equal to any of the τs, the output I is small. When, $\lambda = \tau_i$ for some i, I is approximately equal to α_i. So, as λ is gradually increased, there is a series of peaks corresponding to $\tau_i s$, with their associated magnitudes $\alpha_i s$.

B. Type II

The disadvantage of NDR I is that separate copies of the test signal and its reflections are required. This will require a directional coupler to separate the signals, which requires relatively large and costly circuit elements. There is also the potential that the directional coupler would limit the bandwidth of the signal, but for the range we are currently using, this has not been a problem. A simpler alternative is a second type of NDR, the NDR II shown in Fig. 2. NDR II analyzes the superposition of

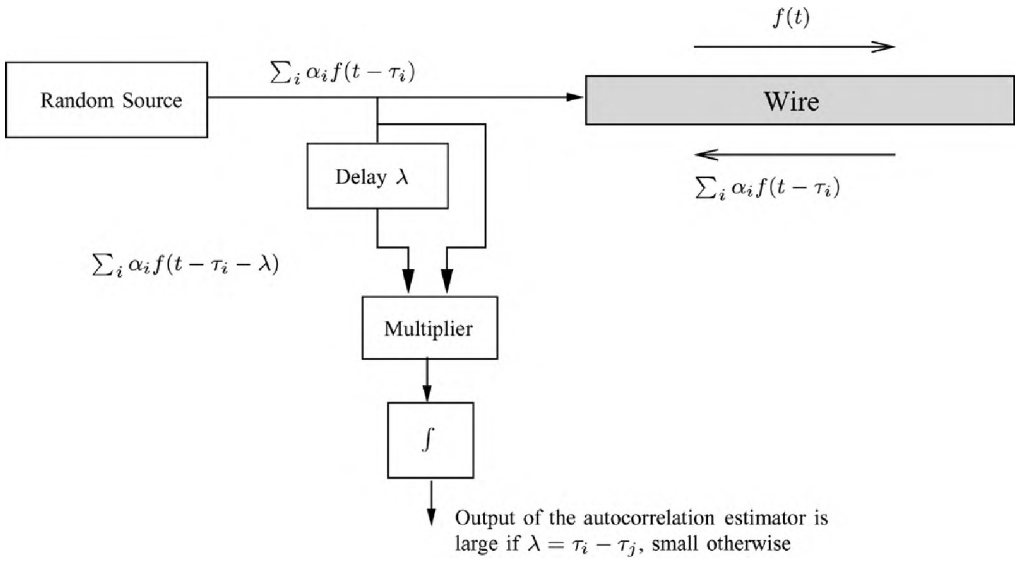

Fig. 2. NDR II block diagram.

the test signal and its reflections, so does not need the directional coupler to separate the signals.

The derivation of the NDR II correlation is similar to that for NDR I. Assume there are N reflection paths, each with a delay τ_i and returned signal strength α_i. For convenience, let the magnitude and delay of the test signal be $\alpha_0 = 1$ and $\tau_0 = 0$. The mixture of the signals is $\sum_{i=0}^{N} \alpha_i f(t-\tau_i)$. Multiplying the signal mixture with a manually delayed version of itself and integrating for length of time T, one will have

$$\begin{aligned} I &= \int_{-T}^{T} \left(\sum_{i=0}^{N} \alpha_i f(t-\tau_i)\right)\left(\sum_{j=0}^{N} \alpha_j f\left(t-(\lambda+\tau_j)\right)\right) dt \\ &= \sum_{i=0}^{N}\sum_{j=0}^{N} \alpha_i\alpha_j \int_{-T}^{T} f(t-\tau_i) f\left(t-(\lambda+\tau_j)\right) dt \\ &= 2T \sum_{i=0}^{N}\sum_{j=0}^{N} \alpha_i\alpha_j \phi_{f_T}(\tau_i-\tau_j-\lambda) \\ &\approx 2T \sum_{i=0}^{N}\sum_{j=0}^{N} \alpha_i\alpha_j \delta(\tau_i-\tau_j-\lambda). \end{aligned} \tag{9}$$

Whenever $\lambda = \tau_i - \tau_j$, I has a peak. Since $\lambda \geq 0$, only peaks corresponding to $\tau_i \geq \tau_j$ occur. There are a maximum of $(N/2)(N+1)+1$ peaks, including the peak at zero.

NDR II returns not only the delays τ_i, but also the differences of the delays ($\tau_i - \tau_j$, etc.). The drawback of NDR II is that it is difficult to distinguish which peaks correspond to the actual delays and which peaks correspond to the differences between the delays. Particularly problematic are cases where the actual and differenced peaks overlap or partially overlap. These limitations can be reduced or eliminated using curve fitting algorithms to identify the peaks and intelligent algorithms to "decode" the network topology based on the observed peaks. Similar algorithms are required for both NDR I and II, and do not in general favor one method over the other. Except for very simple networks where the multiple reflection peaks are intuitive, these algorithms are beyond the scope of this paper and will be covered in later publications. It should be noted that this decoding of multiple peaks is common to all types of reflectiometry including TDR, FDR, STDR, and SSTDR as well as NDR.

IV. Performance Analysis

There are two major factors affecting the performance of NDR. First, it is shown in (3) that the autocorrelation function NDR uses is only an approximation of the "true" autocorrelation function. The approximation is only "good" when the observed interval of $f(t)$ is large [12]. If $f(t)$ is available in the interval $(-\Omega, \Omega)$ which has a finite duration, then, as defined in (3)

$$\phi_{f_T}(\tau) = \frac{1}{2T-|\tau|} \int_{-T+\frac{|\tau|}{2}}^{T-\frac{|\tau|}{2}} f\left(t+\frac{\tau}{2}\right) f\left(t-\frac{\tau}{2}\right) dt. \tag{10}$$

Because $f(t)$ is time invariant, the mean of its autocorrelation estimator is $E(\phi_{f_T}(\tau)) = \phi_f(\tau)$. Furthermore, let $\psi(t) = f(t+(\tau/2))f(t-(\tau/2))$, and the variance of the estimator is given by [12]

$$\sigma^2_{\phi_{f_T}}(\tau) = \frac{1}{2T-|\tau|} \int_{-2T+|\tau|}^{2T-|\tau|} C(\alpha)\left(1-\frac{|\alpha|}{2T-|\tau|}\right) d\alpha \tag{11}$$

where $C(\alpha)$ is the autocovariance of $\psi(t)$. Since $f(t)$ is unit powered, $C(\alpha)$ must be absolute integrable, that is,

$$\int_{-\infty}^{\infty} |C(\alpha)|\, d\alpha < \infty \tag{12}$$

which implies

$$\lim_{(2T-|\tau|)\to\infty} \sigma^2_{\phi_{f_T}(\tau)} = 0. \tag{13}$$

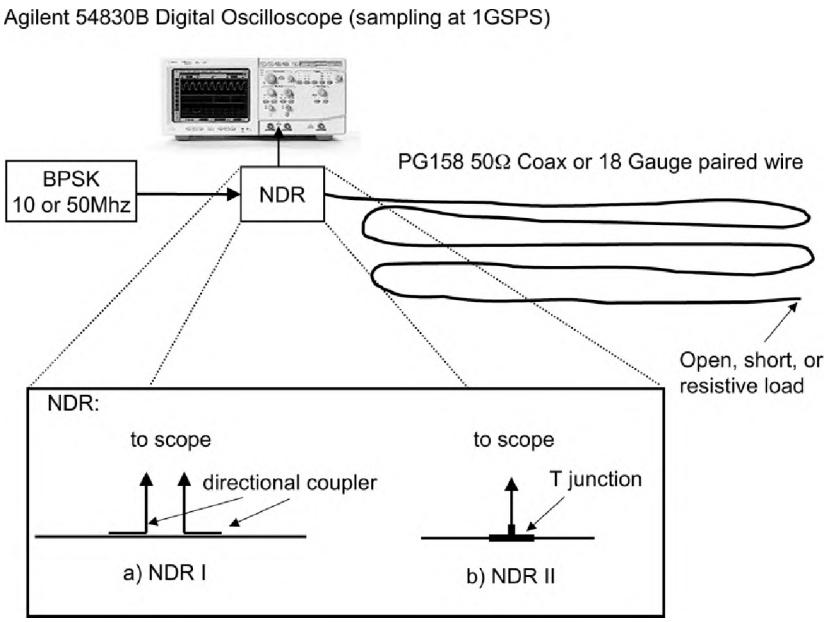

Fig. 3. Setup of the test system.

In other words

$$\lim_{(2T-|\tau|)\to\infty} \phi_{f_T}(\tau) = \phi_f(\tau) \tag{14}$$

for every τ. So, if $2T - |\tau|$ is sufficiently large, the autocorrelation estimator defined above gives very good estimation. However, from (11), if T is fixed, then no matter how large it is, the autocorrelation estimation only works when $\tau \ll T$.

The above derivation not only shows that a long integration interval is required for a good autocorrelation estimator, but also provides a hint of what kind of NDR performance degradation is observed if an autocorrelation estimation with insufficient integration interval is used. NDR determines the wire length by locating the maximum peak from the autocorrelation estimator. A "signal-to-noise" ratio defined based on the ratio between the highest peak for $\phi_f(0)$ and the other peaks is derived naturally. Equation (11) provides a measure of how high the other peaks can be, and at the same time how much the height of the main peak may be reduced. It may therefore be used as a measure of performance.

Second, the detection resolution of NDR I and NDR II is directly related to the bandwidth of the test signal. This is because the autocorrelation function and power spectral density are Fourier transformation pairs. The "narrower" the bandwidth of the test signal, the "wider" the span of its autocorrelation function. The resolution of NDR I and NDR II is directly dependent on the shift un-correlateness of the autocorrelation function. In the above discussion, we assume the test signal is "basically" shift orthogonal, that is, it has infinite bandwidth. However, in real applications, the bandwidth of a test signal is finite. As a result, its autocorrelation function is not a perfect delta function, and therefore one cannot have infinite accuracy with NDR measurements. On the other hand, there are properties of the autocorrelation function that one may explore for one's use. For example, for any physically realizable signals, their autocorrelation functions are even functions, and by using this symmetrical property, the resolution may be improved.

V. Implementation and Testing of NDR

In order to verify the validity of the simulations, NDR was implemented with a high-speed digital oscilloscope. The experimental setup is shown in Fig. 3, where a BPSK data source is connected to an NDR. Depending on whether NDR I or NDR II is being tested, the NDR device consists of a pair of directional couplers or a T junction respectively.

The high-speed digital oscilloscope is sampling at 1 Gs per second (GSPS) for all tests. The sampling interval is 1 ns. For a propagation speed of two thirds the speed of light, 1 ns will be equivalent to around 4 inches of wire. The oscilloscope holds 131 072 sample points, which corresponds to 0.13 ms of sampling duration or more than 40000 feet of wire. In practice, a more realistic limit on maximum wire length comes from evaluation of the attenuation of the signal on the wire found in Section V-A. The sample points are used to estimate the correlation functions as in (8) and (9).

A. Measurement of Discontinuity

The estimation of the correlation functions for NDR I and II is plotted in Figs. 4 and 5, respectively. The magnitude of the impedance discontinuity, which controls the reflection coefficient will also control the magnitude of the correlation peaks. This is shown in Fig. 4 for short circuits, 20-, 50-, 100-, and 1000-Ω resistive loads and open circuits on RG58 (50 Ω) coax. Fig. 5 shows similar results for an NDR II. The magnitude of the peaks is also controlled by the attenuation curve of $Ae^{\beta d}$, where A is a scaling constant, β is an attenuation constant depending on the test wire, and d is the distant of the discontinuity from the NDR. The attenuation curve can also help us to determine the maximum length of a wire NDR can measure. For RG58 coax, we can reach an estimated wire length of 1800 feet before the magnitude of the peak for open or short circuits drops below one tenths of it original height. A binary phase shift keying (BPSK) signal with a 50-MHz chip rate is the data on

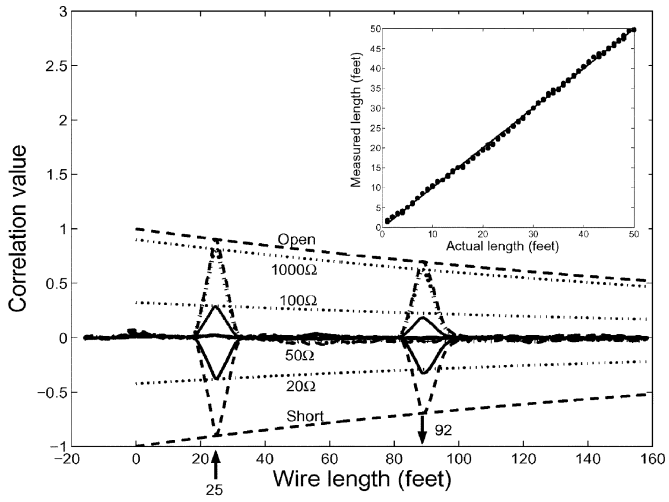

Fig. 4. Measured correlation of NDR I for 25- and 92-foot wire, with a variety of terminations on the wire. Inset shows excellent linearity between the calculated and actual wire lengths.

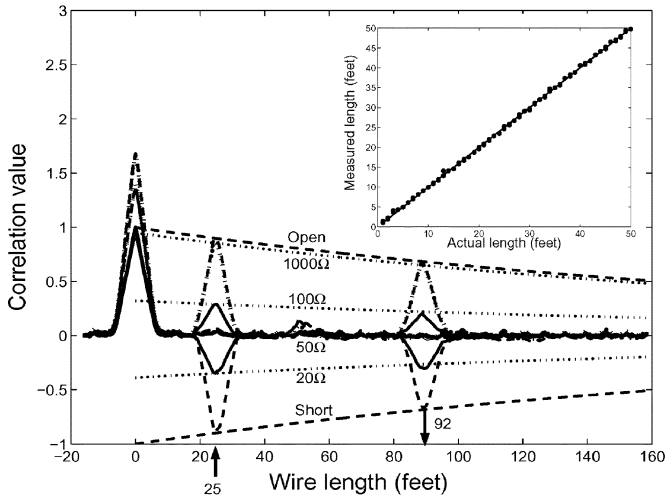

Fig. 5. Measured correlation of NDR II for 25- and 92–foot wire with a variety of terminations on the wire. Inset shows excellent linearity between the calculated and actual wire lengths.

the line. From these plots, it is clear that NDR is capable of detecting impedances below 20 Ω or above 100 Ω, intermittent or otherwise. Faults on this order are substantial damage to the wire. Small chafes or frays, which only represent a few ohms of change in impedance could not be detected. It is critical to test the wire while it is live so that intermittent conditions—a drop of water on a radial crack, for instance- would appear as significant impedance discontinuities, albeit momentarily, as opposed to the small impedance changes they will be in a static condition.

The peaks of the estimated correlation functions are used to determine the length of the wire. On the upper right-hand corner of Figs. 4 and 5 are the estimated length versus the actual length of the wire for NDR I and NDR II respectively. The wire tested is 18 gauge paired wire (Carol 02 301.R5.02 18/2 spt 1), cut in 1-foot increments. Five different readings were taken for both NDR I and II at each measured length. The standard deviation σ for all the tests are 0.21 and 0.29 feet for NDR I and II, respectively, for an integration length of 131 000 points.

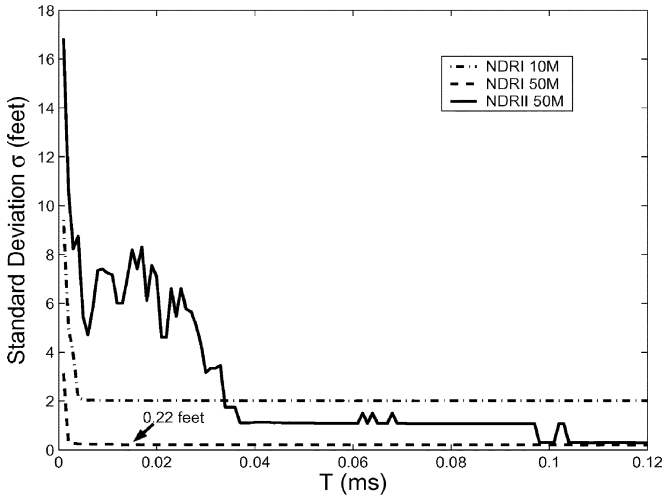

Fig. 6. Integration interval versus performance.

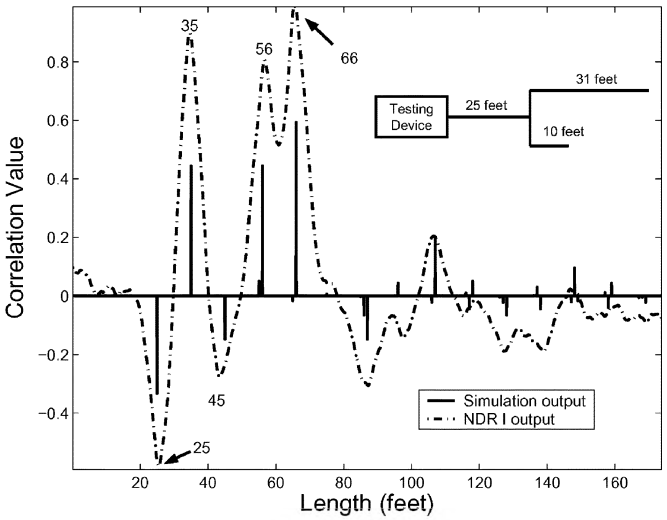

Fig. 7. Testing of NDR I for a branched wiring network.

B. Relationship Between Integration Interval and Performance

It was shown in Section IV that the integration interval T must be significantly larger then the time shift τ in order to have a good correlation estimation. However, we must minimize the integration interval to shorten the detection time for intermittent faults. Typically, an intermittent fault lasts for a few (5–20) milliseconds. We tested three different systems to compare required integration time T—NDR I with 10- and 50-MHz BPSK, and NDR II with 50-MHz BPSK. It is shown in Fig. 6 that both NDR I systems need only 0.005 ms of integration per sample to reach their measurement error floor of 0.2 and 2 feet standard deviation, respectively, while NDR II needs 0.037 ms to reach an error margin of 1.1 feet and 0.1 ms for 0.2 feet. For a typical scan of 256 points, the NDR I system will need a total of 1.28 ms, and the NDR II system will need a total of 9.5 ms for a 1.1-ft error margin. The error margin can be further improved by using broader band (white noise) data and broader band sampling and coupling hardware. Also, from Fig. 6, we can observe that the error floor for 10-MHz NDR I is around ten times larger then that of 50-MHz NDR I. This agrees with our analysis in Section IV.

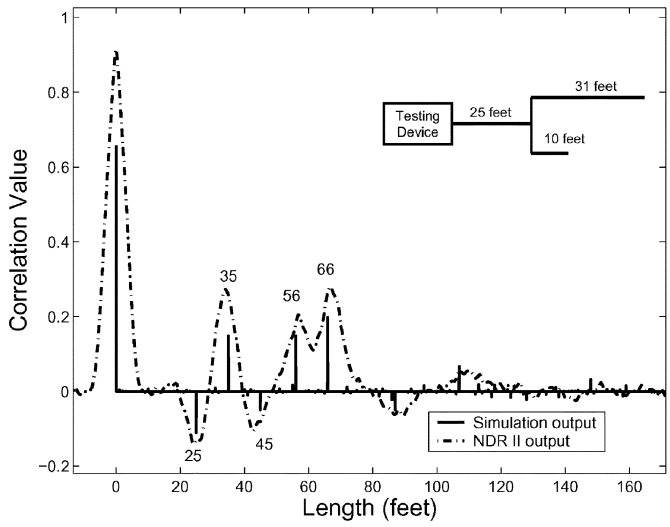

Fig. 8. Testing of NDR II for a branched wiring network.

C. Branched Networks

Use of NDR on wire systems with multiple reflections produces multiple peaks as shown in Figs. 7 and 8. Along with the measured correlation functions, we also plot the simulated impulse response of the wire network. We can see that both NDR I and II are able to distinguish the reflections when they are sufficiently separated. As the peaks get closer, they becomes overlapping, and the delay becomes indistinguishable. Special algorithms are being developed to handle this situation, and are beyond the scope of this paper.

VI. Conclusion

The family of NDR, which use the noise (or any other high frequency uncorrelated signal) on wires to measure their length has been proposed as a new class of reflectometry sensors for locating faults on wires. It could be extended to finding other lengths/distances of interest such as radar or location of users within wireless communication networks. Both NDR I and NDR II utilize the properties of the autocorrelation functions of random signals. NDR uses existing signals on the wire and is totally "quiet" to other users on that wire. Generally, the accuracy of NDR is related to the bandwidth of the testing signal and the integration time of the correlator. NDR I requires separation between the testing signal and its reflection (using directional couplers which limit the bandwidth of the system), and returns the path delays directly. On the other hand, NDR II does not require the testing signal to be separated from its reflection and results in a simpler implementation. The drawback of NDR II is the increased difficulty in analysis to determine the actual time delays, because NDR II returns the path delays plus their sums and differences. Because of not needing to separate the test signal and its reflections, the detection can be done totally nonintrusively for NDR II. The theoretical analysis of the NDR method anticipates its feasibility, which was further demonstrated with actual measurements. Like other reflectometry methods, NDR is only able to locate impedance discontinuities that are significant enough to return a detectable reflected signal. Chafes and frays are therefore undetectable with this or other reflectometry methods. Being able to test the wire while it is live gives NDR two sizable advantages. First, intermittent short circuits (arcs fault) are detected as if they are short circuits (which produce sizable reflection), albeit only momentarily. Intermittent open circuits can be similarly detected. After the fact, either of these conditions commonly returns to being little more than a chafed insulation or loose connection that is too small to detect. Another advantage of running live is that a dynamic baseline can be maintained. Comparison with this baseline may enable NDR to locate faults that would be smaller than those that could be detected with a static baseline. This particular aspect of the method is still under investigation, as little is known about the impedance profile of intermittent faults (other than intermittent opens/shorts) or the noise level that would be observed on a realistic dynamic baseline. In conclusion, the NDR is an important reflectometry method, that has been demonstrated to be capable of locating intermittent faults on live wires utilizing the broadband signals and/or noise that is already on the wire itself. This totally passive method could be used where data integrity issues are vital and/or stealth is required.

References

[1] C. Furse and R. Haupt, "Down to the wire [aircraft wiring]," *IEEE Spectr.*, vol. 38, no. 2, pp. 34–39, Feb. 2001.

[2] N. A. Mackay and S. R. Penstone, "High-sensitivity narrow-band time-domain reflectometer," *IEEE Trans. Instrum. Meas.*, vol. 23, no. 2, pp. 155–158, Jun. 1974.

[3] C. S. Chen, L. E. Roemer, and R. S. Grumbach, "Cable diagnostics for power cables," in *Proc. IEEE Annual Conf. Elect. Eng. Problems Rubber Plastic Industries*, Apr. 1978, pp. 20–22.

[4] G. J. Conroy, "Cable fault locating by electronic means," in *Proc. Mines Technol. Transfer Semin, Mine Power Distrib*, Mar. 1995, pp. 104–114.

[5] N. G. Paulter, "Long-term repeatability of a tdr-based printed wiring board dielectric constant measurement system," *IEEE Trans. Instrum. Meas.*, vol. 47, no. 6, pp. 1469–1473, Dec. 1998.

[6] C. Furse, Y. C. Chung, R. Dangol, M. Nielsen, G. Mabey, and R. Woodward, "Frequency-domain reflectometry for on-board testing of aging aircraft wiring," *IEEE Trans. Electromagn. Compat.*, vol. 45, no. 2, pp. 306–315, May 2003.

[7] C. Furse, P. Smith, M. Safavi, and C. Lo, "Feasibility of spread-spectrum reflectometry for location of arcs on live wires," *IEEE Sensors J.*, to be published.

[8] K. Jones *et al.*, "Adapative apparatus for transmission line analysis," U.S. Patent App. 20 020 169 585, Mar. 2002.

[9] V. Taylor and M. Faulkner, "Line monitoring and fault location using spread spectrum on power line carrier," in *Proc. IEE Gener. Transm. Distrib.*, vol. 143, Sep. 1996, pp. 427–434.

[10] J. Peyton and Z. Peebles, *Probability, Random Variables, and Random Signal Principles*, 3rd ed. New York: McGraw Hill, 1993.

[11] P. Pendayala, "Development of algorithms for accurate wire fault location using spread-spectrum reflectometry," Master's thesis, University of Utah, Salt Lake City, UT, May 2004.

[12] A. Papoulis, *Signal Analysis*. New York: McGraw-Hill, 1977.

Chet Lo (S'95–M'02) received the B.A. degree in physics/mathematics, the M.S. degree in mathematics, the M.S. degree in electrical engineering, and the Ph.D. degree in electrical engineering from Utah State University, Logan, in 1993, 1997, 1998, and 2001 respectively.

He is currently with the Department of Electrical and Computer Engineering, University of Utah, Salt Lake City. His current research interests include wire health monitoring, reflectometry theory, and adaptive signal processing for branched wiring system identification.

Dr. Lo was awarded the Best International Teaching Associate of The Year and was the winner of the Best Research Paper Competition on Scholar Day at Utah State University.

Cynthia Furse (S'85–M'87–SM'99) received the Ph.D. degree in electrical engineering from the University of Utah, Salt Lake City, in 1994.

She is the Director of the Center of Excellence for Smart Sensors, University of Utah, and an Associate Professor in the Electrical and Computer Engineering Department. The Center focuses on imbedded sensors in complex environments, particularly sensors for anomalies in the human body and aging aircraft wiring. She has directed the Utah "Smart Wiring" program, sponsored by NAVAIR and USAF, for the past seven years. She teaches electromagnetics, wireless communication, computational electromagnetics, microwave engineering, and antenna design.

Dr. Furse was the Professor of the Year in the College of Engineering at Utah State University, Logan, for the year 2000, Faculty Employee of the year 2002, a National Science Foundation Computational and Information Sciences and Engineering Graduate Fellow, IEEE Microwave Theory and Techniques Graduate Fellow, and President's Scholar at the University of Utah. She is the Chair of the IEEE Antennas and Propagation Society Education Committee, and Associate Editor of the IEEE TRANSACTIONS ON ANTENNAS AND PROPAGATION.